The Journal of Systems and Software 84 (2011) 2005–2012

Contents lists available at ScienceDirect

The Journal of Systems and Software

journal homepage: www.elsevier.com/locate/jss

Measuring air quality in city areas by vehicular wireless sensor networks

Shu-Chiung Hu[a,*], You-Chiun Wang[b], Chiuan-Yu Huang[a], Yu-Chee Tseng[a]

[a] Department of Computer Science, National Chiao Tung University, Hsin-Chu 300, Taiwan
[b] Department of Computer Science and Engineering, National Sun Yat-Sen University, Kaohsiung 80424, Taiwan

ARTICLE INFO

Article history:
Received 17 February 2011
Received in revised form 7 May 2011
Accepted 16 June 2011
Available online 23 June 2011

Keywords:
Micro-climate monitoring
Opportunistic communication
Pervasive computing
Vehicular sensor network
Wireless sensor network

ABSTRACT

This paper considers a *micro-climate monitoring* scenario, which usually requires deploying a large number of sensor nodes to capture environmental information. By exploiting *vehicular sensor networks* (*VSNs*), it is possible to equip fewer nodes on cars to achieve fine-grained monitoring. Specifically, when a car is moving, it could conduct measurements at different locations, thus collecting lots of sensing data. To achieve this goal, this paper proposes a VSN architecture to collect and measure air quality for micro-climate monitoring in city areas, where nodes' mobility may be uncontrollable (such as taxis). In the proposed VSN architecture, we address two network-related issues: (1) how to adaptively adjust the reporting rates of mobile nodes to satisfy a target monitoring quality with less communication overhead and (2) how to exploit opportunistic communications to reduce message transmissions. We propose algorithms to solve these two issues and verify their performances by simulations. In addition, we also develop a ZigBee-based prototype to monitor the concentration of carbon dioxide (CO_2) gas in city areas.

1. Introduction

After the industrial revolution, the burning of fossil fuels and many human activities have significantly increased the concentration of carbon dioxide (CO_2) year by year. It is widely concluded that the increase of the CO_2 concentration is a major reason to cause global warming. Therefore, it would be quite interesting to understand how the CO_2 concentration changes over temporal and spatial domains at a very fine-grained size. This is generally related to *micro-climate monitoring*, which intends to collect environmental information in a quite small scale (for example, one measurement per 10 m).

In this paper, we aim at micro-climate monitoring in city areas by using *vehicular sensor networks* (*VSNs*). We consider sensor nodes whose mobility may be uncontrollable (for example, equipping sensor nodes on taxis or buses). Micro-level monitoring usually requires deploying a large number of sensor nodes. However, through mobility, a sensor node can conduct measurements at many different locations, thereby relaxing the demands on the number of sensor nodes. Still, this problem poses several challenges: (1) calibration of sensing data, (2) management and operation of VSNs, and (3) collection and presentation of sensing data.

Among the above challenges, we would like to particularly address two *network-related* issues: (1) how to adaptively adjust the reporting rates of mobile nodes to satisfy a target monitoring quality while reducing the communication overhead and (2) how to exploit opportunistic communications to reduce message transmissions. For example, in a crowded area with many cars carrying sensor nodes, we can reduce the reporting rates of some nodes to reduce possible duplication. On the other hand, at those fields where the CO_2 concentration changes dramatically, a node may need to increase its reporting rate to improve the accuracy. For opportunistic communications, a node may pass its sensing data to a neighbor which is going to submit a report shortly. Also, a node which just arrives at an area may inquire a neighbor (instead of the central server) the required reporting rate inside the area.

We propose a VSN architecture to measure air quality for micro-climate monitoring in city areas, where the CO_2 concentration may change over different regions and the number of mobile nodes could be large. We design two message-efficient algorithms to address issue (1). In particular, the sensing field is divided into regular grids. Each grid can impose its own reporting rate on the nodes within its region. The first algorithm tries to measure the changes of the CO_2 concentration inside a grid and then determine the expected number of reports to be collected within that region. On the other hand, the second algorithm tries to use the changes of the CO_2 concentration and the number of cars inside a grid to determine the expected reporting rate. To address issue (2), we allow a node to collect information and submit reports by taking advantage of its neighbors opportunistically.

* Corresponding author.
E-mail addresses: schu@cs.nctu.edu.tw (S.-C. Hu), ycwang@cse.nsysu.edu.tw (Y.-C. Wang), chiuanyu@cs.nctu.edu.tw (C.-Y. Huang), yctseng@cs.nctu.edu.tw (Y.-C. Tseng).

0164-1212/$ – see front matter © 2011 Elsevier Inc. All rights reserved.
doi:10.1016/j.jss.2011.06.043

We verify our results through simulations as well as a real prototype. Specifically, we develop a ZigBee-based car network to monitor the CO_2 concentration in Hsinchu City, Taiwan. In our prototype, a car is equipped with a CO_2 sensor, a GPS (global positioning system) receiver, and a GSM (global system for mobile communications) module, which form a ZigBee-based intra-vehicle wireless network. These vehicular nodes roam inside the area of interest and periodically report their sensing data through GSM short messages. These reports are collected by a central server, which shows the monitoring result via Google Maps (2010).

The rest of this paper is organized as follows. Section 2 surveys related work. Section 3 presents the proposed VSN architecture and our algorithms. Section 4 gives our simulation results. Our prototyping results are presented in Section 5. Section 6 concludes this paper.

2. Related work

Wireless sensor networks (*WSNs*) have been widely adopted in surveillance and monitoring applications. For example, He et al. (2006) adopt WSNs to provide a safe and secret way for acquiring information from hostile targets in military surveillance missions. The OceanSense project (Liu et al., 2008) deploys a submarine WSN to collect oceanic data such as temperature and sea depths, while Li and Liu (2007) deploy an underground WSN to monitor coal mines. To forecast volcano eruptions, Werner-Allen et al. (2005, 2006) deploy refractory sensors around active volcanos. WSNs are also deployed to monitor civil infrastructures such as buildings and railway bridges (Xu et al., 2004; Chebrolu et al., 2008). In Wang et al. (2003) and Chebrolu et al. (2007), multi-layer WSNs are proposed to improve the network bandwidth and reduce energy consumption under various surveillance applications. These works all require a large number of static sensor nodes in the sensing field.

Recently, the concept of mobility is introduced to WSNs by dispatching sensor nodes to conduct various missions, such as replacing broken nodes and reacting to the events (Cao et al., 2006; Wang et al., 2010). Such WSNs are usually called *mobile WSNs*. Since sensor nodes are more maneuverable, mobile WSNs have been adopted in vorious surveillance applications. For example, iMouse (Tseng et al., 2007) develops a hybrid WSN consisting of static and mobile sensors for indoor surveillance, where mobile sensors can be dispatched to analyze the abnormal events reported from static sensors. SensorFlock (Allred et al., 2007), an airborne WSN composed of various micro-aerial sensing devices, is designed to analyze toxic plume and storm dynamics to build a three-dimensional view of the atmospheric system. ZebraNet (Juang et al., 2002) is developed to track zebras' migration in Africa, where sensor nodes are equipped on zebras to record their movements and interactions. It can be observed that in the above systems, sensor nodes should be equipped on either specially-made mobile carriers or animals.

Several studies suggest adopting common vehicles such as cars and bicycles as the mobile carriers of sensor nodes to reduce the deployment cost. For example, by equipping multiple types of sensor nodes such as microphones and cameras on bicycles, Eisenman et al. (2009) allow cyclists to help collect road information along some predefined routes. In Kargupta et al. (2004), cars are equipped with vehicular sensors and GPS receivers to conduct car-health monitoring and collect driver habits. In Lee et al. (2006), cameras and chemical sensors on vehicles are used to monitor pollution along streets and vehicles may exchange their monitoring data when they meet each other. In CarTel (Hull et al., 2006), each car is equipped with a GPS receiver to trace its route, a camera to monitor road conditions, and a wireless interface to report data to a central server. These reports can be used for future route planning. Similar to these studies, our work develops a VSN architecture for micro-climate monitoring in city areas. In addition, we address two network-related issues in such an environment. Different from Eisenman et al. (2009), Kargupta et al. (2004), and Hull et al. (2006), we aim at adaptively adjusting the reporting rates of vehicles to balance between the monitoring accuracy and the communication cost. Note that a higher reporting rate improves the monitoring accuracy but incurs a higher message cost (here we adopt GSM short messages), and vice versa. Therefore, our goal is to satisfy a target monitoring quality by minimizing the communication overhead. In addition, we exploit opportunistic communications to aggregate vehicles' reports to further reduce the message cost.

3. VSN-based solutions for micor-climate monitoring

Fig. 1 shows the proposed VSN architecture for micro-climate monitoring. The system consists of some vehicular sensor nodes, a monitoring server, and cellular networks. Each vehicular sensor node (or simply called *vehicular node* or *node*) consists of a central unit and an external unit. The central unit is placed inside the car, while the external unit is attached outside the car so as to collect environmental data. The central unit is connected to a cellular interface (for example, 2G/3G/3.5G), a GPS receiver, and two wireless interfaces. The external unit is connected to a wireless interface and some sensors depending on the application. Here, we consider monitoring CO_2 concentration, so a CO_2 sensor is needed. The central and external units communicate with each other through their

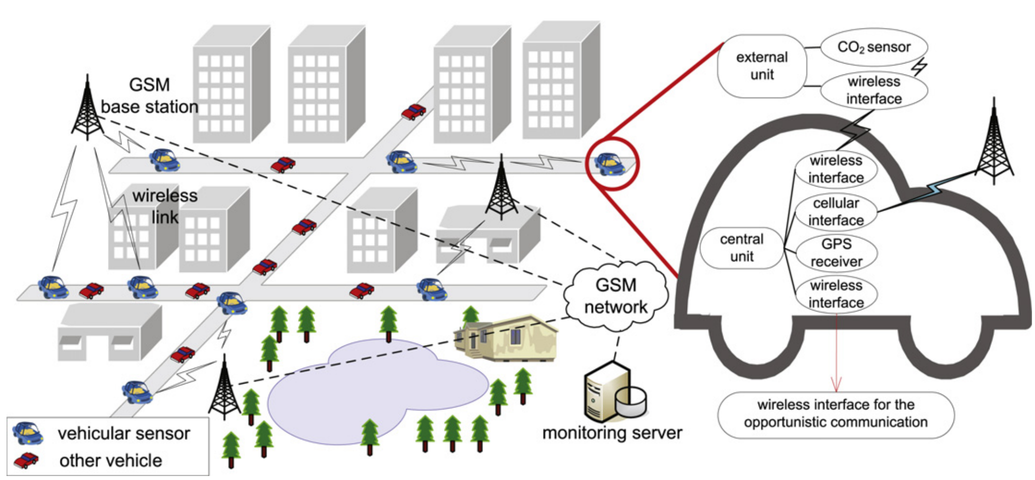

Fig. 1. The proposed VSN architecture for micro-climate monitoring.

wireless interfaces (in this paper we adopt ZigBee). Periodically, the central unit collects the detected CO_2 concentration from the external unit and reports the data, together with its current location, to the monitoring server. The monitoring server then collects all data in each predefined time frame and renders the result on a map (in this paper, we adopt Google Maps (2010).

To reduce the communication overhead, the central unit of a vehicular node can also form an ad hoc network with nearby nodes via their wireless interfaces (for example, Wi-Fi). Such an ad hoc network would allow opportunistic communications among vehicular nodes. Therefore, a node can collect information from its neighbors and help relay other nodes' sensing data to the monitoring server.

In this paper, we consider two network-related issues in the micro-climate monitoring problem. First, since a city area is considered, not only the CO_2 concentration but also the density of vehicular nodes may change dramatically from time to time. Thus, one may need to impose different reporting rates for mobile nodes in different subareas. We call this the *dynamic reporting rate* (*DRR*) *problem*, whose goal is to reduce the communication overhead on the cellular networks while achieving certain monitoring quality. Second, to further reduce the reporting overhead, we consider the possibility of opportunistic communications. When nodes help relay each other's reports, some sort of data aggregation can be achieved. We assume that each report has a deadline by which time it has to be submitted to the server so as to provide timely services. We call this the *time-constrained opportunistic relay* (*TOR*) *problem*.

To achieve our goals, the whole sensing field is partitioned into fixed-size grids $G_1, G_2, \ldots, G_n$. For the DRR problem, the monitoring server will impose a reporting rate r_i on all vehicular nodes in grid G_i, $i = 1, \ldots, n$. For the TOR problem, nodes will find out their reporting rates and submit their reports in an opportunistic manner. The monitoring server has a predefined time frame of T seconds. In every T seconds, the server combines all reports that it has collected during that frame and renders the result on a map interface. Below, we present our detailed solutions.

3.1. Solutions to the DRR problem

Since CO_2 concentration is dynamic, we need to determine the expected number of samples to collect from each grid in every time frame based on the record of the previous time frame. The number of samples that we need to collect, however, depends on two factors: (1) the distribution of CO_2 concentration in that area and (2) the number and the distribution of vehicular nodes in that area. Assuming G_i as the target grid, we present two schemes below.

(1) *Variation-based scheme:* Intuitively, a higher reporting rate r_i should be set when the variation of the CO_2 concentration in G_i becomes higher, and vice versa. For example, in Fig. 2, since the CO_2 concentration in grids (2, 4) and (2, 5) fluctuates more quickly than that in other grids, higher reporting rates should be imposed on these two grids. Contrarily, the CO_2 concentration in grids (1, 5) and (2, 6) is more stable, so lower reporting rates could be applied to reduce the amount of transmissions.

From the previous time frame, we can calculate the standard deviation σ_i^{con} of all reported values from G_i and the number of vehicular nodes ν_i that have submitted reports for G_i. We use σ_i^{con} as an index to estimate the number of samples (denoted S_i^{var}) that we expect to receive in the upcoming time frame. We suggest setting S_i^{var} as a linear function of σ_i^{con}:

$$S_i^{var} = a_i^{var} \times \sigma_i^{con} + b_i^{var},$$

where a_i^{var} and b_i^{var} are constants based on the past experience (larger values mean higher monitoring qualities). Note that b_i^{var} indicates the smallest number of reports that we expect to receive. Then, the new reporting rate of G_i can be set to $r_i^{var} = S_i^{var}/\nu_i$.

(2) *Gradient-based scheme:* The previous variation-based scheme has no sense of the locations where samples are collected (that is, two samples collected from different locations of the grid are regarded as the same). For example, for two samples with a fixed amount of concentration difference, if these two samples are taken at very close locations, the change of concentration is regarded as more significant as compared to the case when the two locations farther away from each other. Therefore, the concept of "gradient" can be applied to reflect these factors.

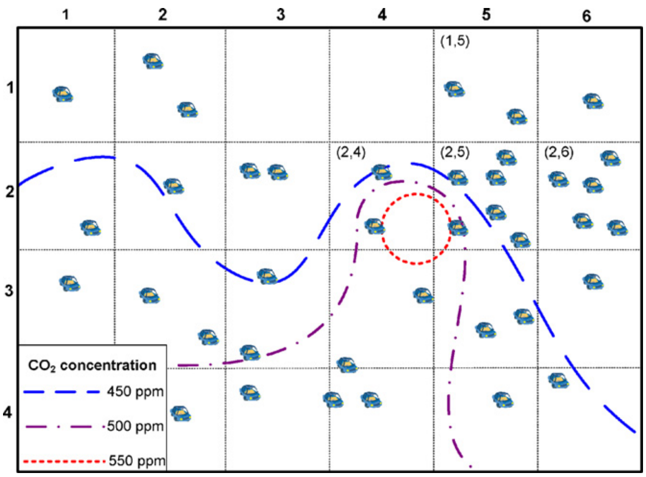

Fig. 2. An example of the reporting rate adjustment.

In this scheme, we collect two sets of samples, one consisting of higher values and one consisting of lower values. We then measure the gradients of all pairs of samples between these two sets. Then, the average gradient is adopted to calculate the new reporting rate. Specifically, let R_{high} and R_{low} be the sets of the top γ% and the bottom γ% of the concentration readings in G_i in the previous time frame, respectively. The gradient of two samples $x \in R_{\text{high}}$ and $y \in R_{\text{low}}$ can be written as

$$\alpha(x, y) = \frac{x - y}{dist(x, y)},$$

where $dist(x, y)$ is the distance of the two locations where x and y are sampled. Then, the average gradient between R_{high} and R_{low} is measured as:

$$\alpha_i^{avg} = \frac{\sum_{x \in R_{\text{high}}, y \in R_{\text{low}}} \alpha(x, y)}{|R_{\text{high}}| \times |R_{\text{low}}|}.$$

Similar to the variation-based scheme, the number of samples S_i^{gra} that we expect to receive in the next time frame can be set as a linear function of α_i^{avg}:

$$S_i^{gra} = a_i^{gra} \times \alpha_i^{avg} + b_i^{gra},$$

where a_i^{gra} and b_i^{gra} are constants based on the past experience. Then, the new reporting rate of G_i can be set as $r_i^{gra} = S_i^{gra}/\nu_i$.

3.2. Solutions to the TOR problem

Through opportunistic communications, a vehicular node can help relay others' reports, estimate its own location when it loses the GPS signal, and inquire the reporting rate when it enters a new grid. Our design also includes a randomness mechanism to

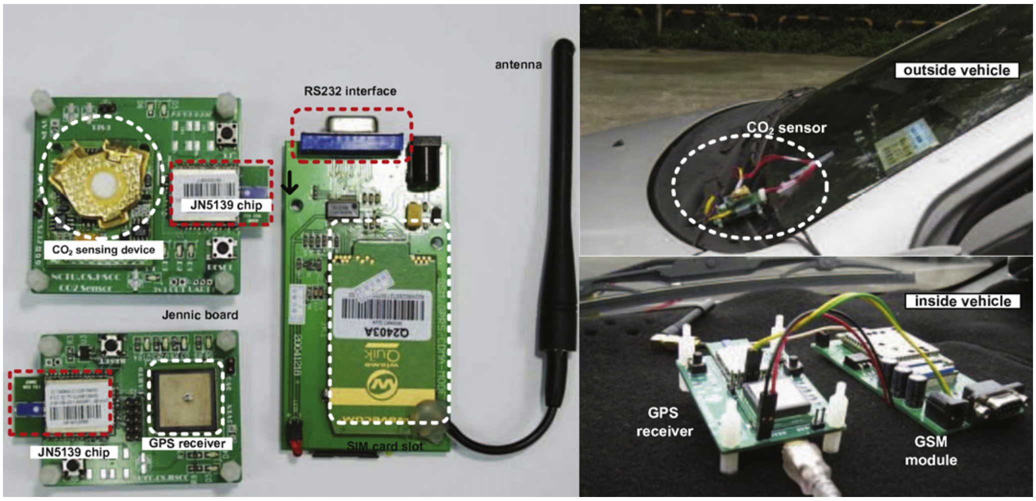

Fig. 3. A snapshot of our prototype.

ensure fairness among nodes when they decide their relaying roles. Note that since GPS is adopted, we assume that nodes are at least roughly time-synchronized. Also, we assume that each node knows the value of T and the due time when the server will render the monitoring result. The details of our solution are listed below:

- Periodically, a node x broadcasts a HELLO packet, through its wireless interface, which contains its current grid ID and its current attraction value att_x, where

$$att_x = rnd_x \times wgt_x,$$

where rnd_x is a random number between 0 and 1 generated by x at the beginning of the current time frame and wgt_x is x's weight variable reflecting the number of sensing reports that x needs to submit to the server so far. Note that wgt_x includes the sensing reports generated by x itself and those that x needs to relay for other nodes.

- When a node does not know the current reporting rate of its current grid after entering a new grid, it first tries to get this information from any neighbor, if possible, through its wireless interface. When the above opportunistic communication is impossible, it then inquires the server through its cellular interface. Then, according to the reporting rate, the node will collect sensing data from its external unit periodically.
- When a node x finds a neighbor y such that $wgt_x < wgt_y$, it tries to send all sensing reports at its hand to y through its wireless interface. On completion of the above operation, x clears wgt_x to zero. On the other hands, y increases its weight wgt_y by wgt_x. If only part of the above process is done before the link between x and y breaks, then these weights are adjusted proportionally. (Note that this step may be extended to multi-hop transmission. However, to reduce complexity and to avoid the ping-pong effect, we choose to only allow one-hop transmission.)
- When x finds that it loses its GPS signal (for example, due to signal blocking), it can estimate its current location through its neighbors' locations. (Note that there are several possibilities (Sheu et al., 2008; Gopakumar and Jocob, 2008) to conduct such an estimation. This is related to localization and is out of the scope of this paper.)
- After the current time frame ends, each node which has a nonzero weight submits all sensing reports at its hand to the server.

The above relaying behavior would allow us to conduct data aggregation to reduce message cost. The reduction ratio is, however, system- and application-dependent. Data aggregation does not affect the measurement accuracy because we assume lossless compression.

4. Simulation results

We develop a simulator in C++ and Matlab to verify the performances of the proposed schemes. Table 1 lists the default parameters in our simulator. Specifically, the monitored region is modeled by a $12.8 \times 12.8\,\text{km}^2$ rectangle, inside which there are 20 horizontal and vertical streets. To simulate a real-road model, vehicular nodes move inside the region following the Manhattan mobility model (Bai et al., 2003), where all nodes move along horizontal or vertical streets. When encountering an intersection, a node determines its moving direction as straight, left turn, and right turn with the probability of 0.5, 0.25, and 0.25, respectively. To keep the total number of vehicular nodes in the region a constant, we do not allow vehicular nodes to move outside the region. Therefore, when a vehicular node reaches the region's boundary, it will turn to an available direction. Vehicular nodes send their reports by GSM short messages. The length of a GSM short message is set to 140 bytes and it costs one dollar. We set frame length T to 600 s.(We will also observe the effect of T in the simulations). The monitored region is divided into 4×4 grids. There are several CO_2 events in this monitored region. The occurrence of CO_2 events follows the Gaussian distribution and each event has a different lifetime. We define the CO_2 event rate as the number of CO_2 events generated every

Table 1
The default parameters of our simulator.

Parameter	Value
Number of streets	20
Area of the monitored region	$12.8 \times 12.8\,\text{km}^2$
Number of grids	16
Number of vehicular nodes	160
Velocity of vehicular nodes	30–60 km/h
CO_2 event rate	$2CO_2$ event
Maximum reporting rate	1/30 report/s
Minimum reporting rate	1/300 report/s
T	600 s
Length of a GSM short message	140 bytes
Cost per GSM short message	1 dollar

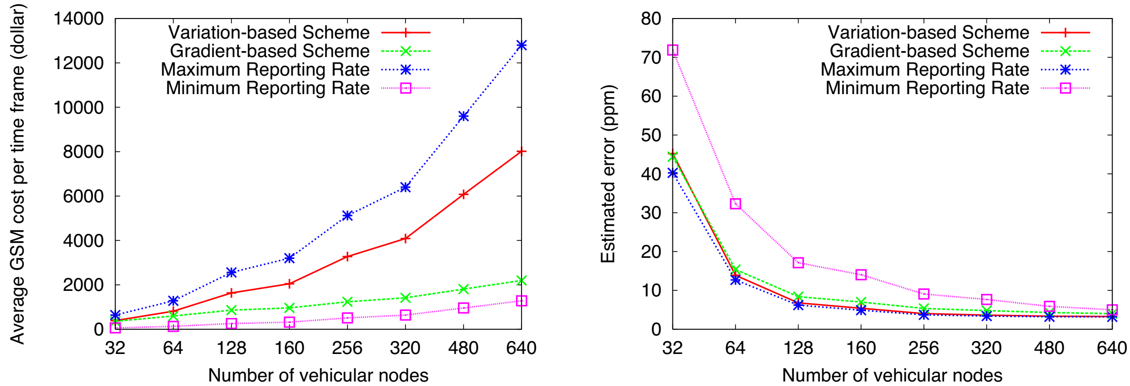

Fig. 4. Comparison of the average GSM short message cost per time frame *T* and the estimated error of CO_2 concentration under different numbers of vehicular nodes.

time frame. We measure the GSM message cost and the estimated error of the CO_2 concentration.

For comparison, we develop two schemes, one using the maximum reporting rate and one using the minimum reporting rate, respectively. Such regular rates are also adopted in Chebrolu et al. (2007) and Juang et al. (2002).

We first observe the effect of different numbers of vehicular nodes on the average GSM message cost per time frame *T* and the estimated error, as shown in Fig. 4. The number of vehicular nodes ranges from 32 to 640. The estimated error is measured by parts per million (ppm). Explicitly, as the GSM message cost increases, the estimated error decreases. Using the maximum reporting rate incurs the highest cost while using the minimum reporting rate incurs the maximum estimated error. Both our variation-based and gradient-based schemes can increase the estimated accuracy while reducing the GSM message cost. The gradient-based scheme can further reduce message transmissions with the expenditure of increasing a small amount of estimated error.

We then observe the effect of vehicular nodes' velocity on the average GSM message cost and the estimated error, as shown in Fig. 5. The velocity range of vehicular nodes are set to [5,25], [35,55], [65,85], [95,115], and [125,145] km/h. It can be observed that this factor has low impact on both GSM message cost and the estimated error. Note that when the node mobility is very low (such as 5-25 km/hr), the benefit of mobility would degrade slightly since a node can only obtain data from nearby locations. In this case, the estimated error will increase.

Fig. 6 shows the impact of the size of the monitored region on the average GSM message cost and the estimated error. The region area ranges from 6.4×6.4 to $102.4 \times 102.4\,km^2$. Changing the region size has almost no effect on the GSM message cost, because the number of vehicular nodes is the same. However, the estimated error increases significantly as the region size increases, because the node density drops fast.

We then vary the number of streets and observe its impact. In Fig. 7, the number of streets ranges from 10 to 100. Changing the number of streets has almost no effect on the GSM message cost because the number of vehicular nodes does not change. When there are very few streets (for example, 10), vehicular nodes can only obtain data from very sparse positions, while results in a higher estimated error.

From Figs. 6 and 7, we can also conclude that node density has the most significant impact on the estimated error.

Fig. 8 shows the effect of different CO_2 event rates on the average GSM message cost and the estimated error. We range the CO_2 event rate from 4 to 24 in every time frame. Because the number of vehicular nodes is constant, changing the CO_2 event rate has almost no effect on the GSM message cost. Interestingly, the GSM message cost of the variation-based scheme suddenly drops when there are 8 CO_2 events. The reason is that the CO_2 event rate in the experiment may not be significant so that smaller reporting rates are set in the variation-based scheme. On the contrary, the CO_2 event rate has significant impact on the estimated error. In particular, since vehicular nodes report almost a constant amount of messages, increasing the CO_2 event rate will result in a higher estimated error. However, both the variation-based and gradient-based schemes can keep quite low estimated errors while reducing the GSM message cost.

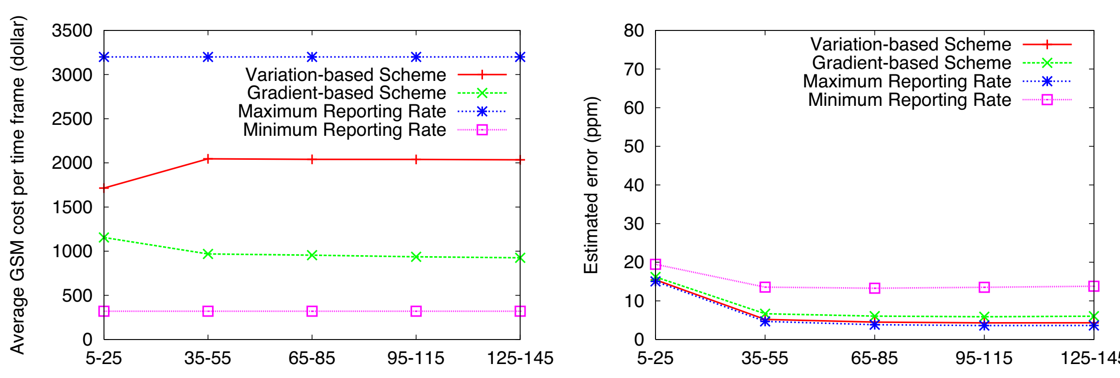

Fig. 5. Comparison of the GSM short message cost per time frame *T* and the estimated error of CO_2 concentration under different velocities of vehicular nodes.

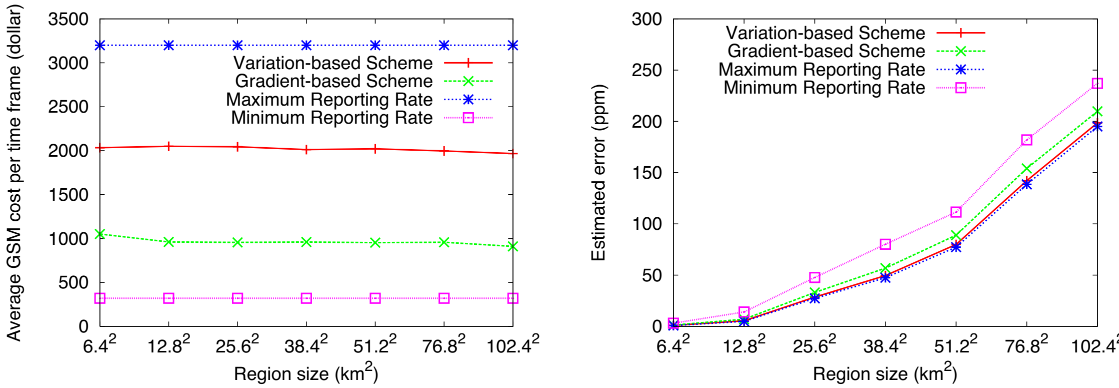

Fig. 6. Comparison of the GSM short message cost per time frame *T* and the estimated error of CO_2 concentration under different sizes of the monitored region.

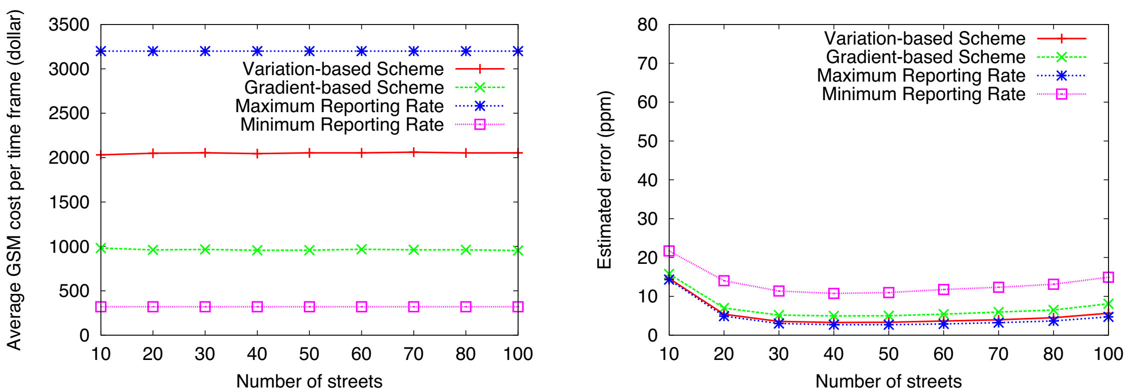

Fig. 7. Comparison of the GSM short message cost per time frame *T* and the estimated error of CO_2 concentration under different numbers of streets.

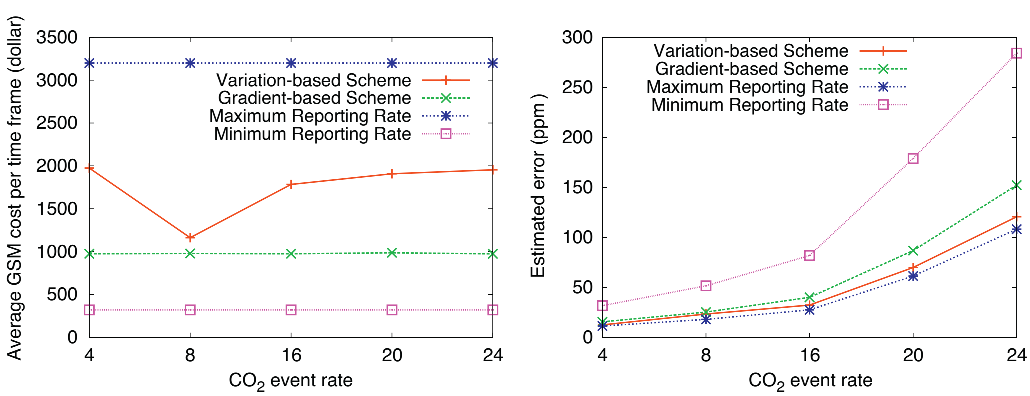

Fig. 8. Comparison of the GSM short message cost per time frame *T* and the estimated error of CO_2 concentration under different variations of CO_2 concentration.

Fig. 9 shows the impact of different time frame length *T* on the average GSM message cost and the estimated error. We vary *T* from 300 to 1050s. As *T* grows, the number of messages per frame increases and the estimated error decreases. For our schemes, the GSM message cost increases less significantly. By using our gradient-based scheme, the increase of the GSM message cost is bounded and the estimated error is reasonable. From Fig. 9, setting *T* to 600 s is a proper choice.

5. Prototyping experiences

We have implemented a prototype of the vehicular sensor node. The hardware components, as shown in Fig. 3 are discussed below.

1. Jennic board: Each Jennic board contains a JN5139 chip (Jennic JN5139, 2008), which has a 32-bit reduced instruction set computing (RISC) processor, a fully-compliant 2.4 GHz IEEE 802.15.4 (IEEE standard for information technology, 2006) transceiver, 192 KB of ROM, and 96 KB of RAM. We adopt the ZigBee protocol (ZigBee specific version, 2006) for inter-board communication.
2. GPS receiver: We adopt the uPatch300 GPS module (uPatch300 module, 2008), which provides geographic location with the maximum tolerant error of 1.8 m. In our prototype, we set the reporting rate to one second.
3. CO_2 sensor: We adopt the H-550EV CO_2 sensor module (H-550EV module, 2008), which samples the CO_2 concentration every three seconds. Its detectable range is from 0 to 5000 ppm with an error range of ±30 ppm. It has response time of 30 s.

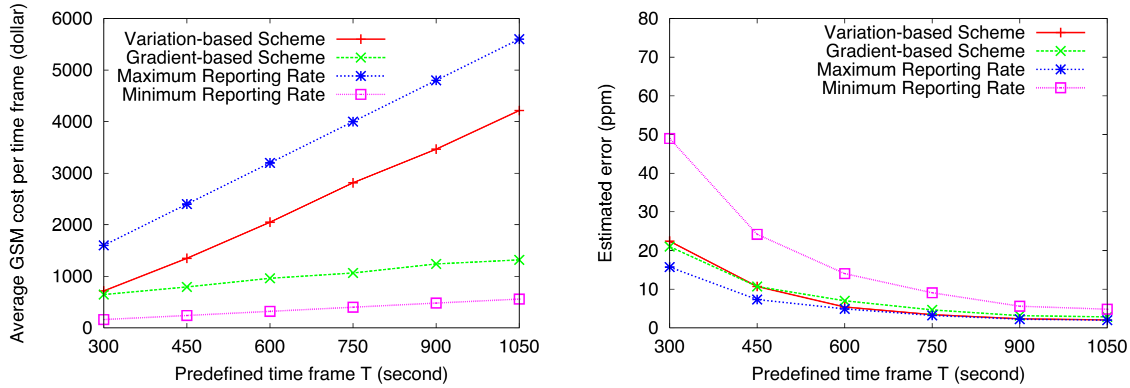

Fig. 9. Comparison of the GSM short message cost per time frame *T* and the estimated error of CO_2 concentration under different time frame *T*.

format:

6 char	6 char	11 char	11 char
time	CO_2 reading	latitude	longitude

example:

184013	000700	02478.8722N	12099.8483E

[message format of a vehicular node]

format:

19 char	19 char	4 char	6 char
top-left latitude & longitude	bottom-right latitude & longitude	rate	expiration

example:

24789715N120996530E	24783968N121004276E	0020	190000

[message format of the server]

Fig. 10. The formats of our GSM short messages.

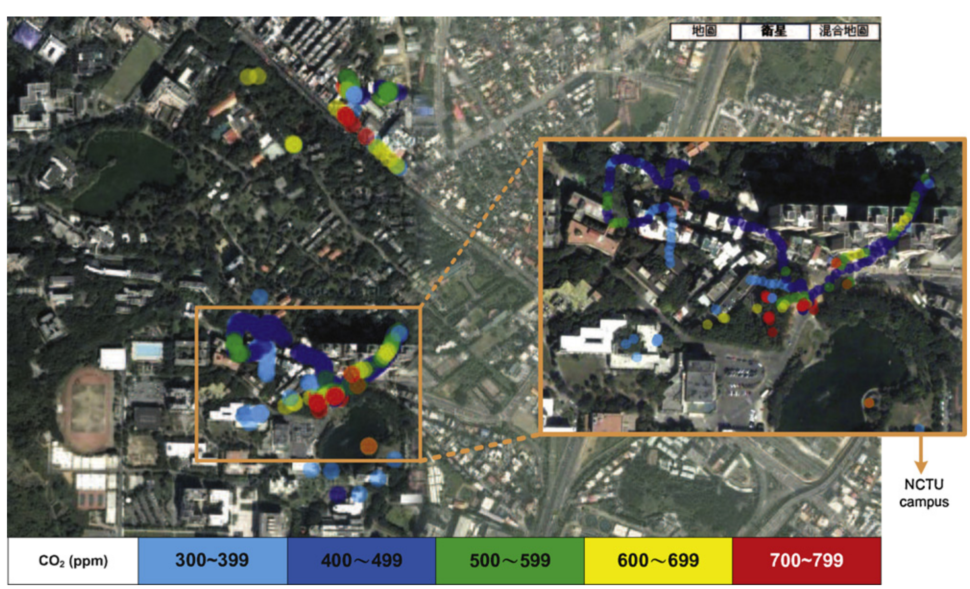

Fig. 11. A snapshot of our user interface.

4. GSM module: We adopt the SIM300 GSM module (SIM300 module, 2008), which supports triband GSM/GPRS communications on 900 MHz, 1800 MHz, and 1900 MHz. It also allows users to transmit GSM short messages.

Fig. 3 shows a snapshots of these components. The CO_2 sensor is installed outside the vehicle, while the GPS receiver and the GSM module are installed inside the vehicle. Each of the GPS receiver and the CO_2 sensor is attached to a Jennic board, so they can communicate with each other through a ZigBee wireless link. The GPS receiver is connected to the GSM module through an RS232 wired interface. The CO_2 sensor reports its readings at a fixed rate to Jennic board inside the vehicle. The Jennic board will then average these readings, combine them with the current location of the vehicle, and report to the monitoring server through GSM short messages. The reporting will follow the requested rate.

Each vehicle reports its current location and monitoring CO_2 concentration through a GSM short message, which follows the format of "time, CO_2 reading, latitude, longitude", as shown in Fig. 10. For example, a GSM short message of "18401300070002478.8722N12099.8483E" means that a vehicle has detected the CO_2 concentration of 700 ppm at the location of 2478.8722° north latitude and 12099.8483° east longitude at time 18:40:13 (hour:minute:second). On the other hand, the server can adjust the reporting rates of vehicles in certain region by sending a GSM message with the format of "latitude and longitude of the top-left point, latitude and longitude of the bottom-right point, new reporting rate, expiration time". For example, a GSM short message of "24789715N120996530E24783968N121004276E0020190000" means that the reporting rates of vehicles inside the rectangle with the top-left point at location (2478.9715N, 12099.6530E) and the bottom-right point at location (2440.8565N, 12100.4276E) should be adjusted to 20 times per hour with expiration time of 19:00:00. The message format of the server is shown in Fig. 10.

Fig. 11 demonstrates a small-scale trial in Hsinchu City. We use Google Maps as the user interface in which we use dots with different colors to represent different CO_2 concentration.

6. Conclusions

In this paper, we have proposed a new architecture based on VSNs for micro-climate monitoring. Through GSM short messages and geographic locations of vehicles, we can use a small number of vehicles to realize fine-grained monitoring in city areas. To balance between the monitoring quality and the message cost, we have designed an adaptive approach to adjust the reporting rates of vehicular sensors according to the variance of sensing readings and the number of vehicular sensors in each grid. We have conducted some simulations to validate our proposed schemes, and also demonstrated the prototype of a ZigBee-based intra-vehicle wireless network for the micro-climate monitoring applications.

Acknowledgements

Y.-C. Tseng's research is co-sponsored by MoE ATU Plan, by NSC grants 97-3114-E-009-001, 97-2221-E-009-142-MY3, 98-2219-E-009-019, and 98-2219-E-009-005, 99-2218-E-009-005, by ITRI, Taiwan, by III, Taiwan, by D-Link, and by Intel.

References

Allred, J., Hasan, A.B., Panichsakul, S., Pisano, W., Gray, P., Huang, J., Han, R., Lawrence, D., Mohseni, K., 2007. Sensorflock: an airborne wireless sensor network of micro-air vehicles. In: Proc. ACM International Conference on Embedded Networked Sensor Systems , pp. 117–129.

Bai, F., Sadagopan, N., Helmy, A., 2003. Important: a framework to systematically analyze the impact of mobility on performance of routing protocols for adhoc networks. In: INFOCOM 2003. Twenty-Second Annual Joint Conference of the IEEE Computer and Communications. IEEE Societies, vol. 2 , pp. 825–835.

Cao, G., Kesidis, G., Porta, T.L., Yao, B., Phoha, S., 2006. Purposeful mobility in tactical sensor networks. Sensor Network Operations.

Chebrolu, K., Raman, B., Mishra, N., Valiveti, P.K., Kumar, R., 2007. Luster: wireless sensor network for environmental research. In: Proc. ACM International Conference on Embedded Networked Sensor Systems , pp. 103–116.

Chebrolu, K., Raman, B., Mishra, N., Valiveti, P.K., Kumar, R., 2008. Brimon: a sensor network system for railway bridge monitoring. In: Proc. ACM International Conference on Mobile systems, Applications, and Services , pp. 2–14.

Eisenman, S.B., Miluzzo, E., Lane, N.D., Peterson, R.A., Ahn, G.S., Campbell, A.T., 2009. Bikenet: a mobile sensing system for cyclist experience mapping. ACM Transactions on Sensor Networks 6, 6:1–6:39.

Google Maps, 2010. http://maps.google.com/.

Gopakumar, A., Jocob, L., January 2008. Localization in wireless sensor networks using particle swarm optimization. In: IET International Conference on Wireless, Mobile and Multimedia Networks , pp. 227–230.

H-550EV module, 2008. http://www.elti.co.kr/.

He, T., Krishnamurthy, S., Stankovic, J.A., Abdelzaher, T., Luo, L., Stoleru, R., Yan, T., Gu, L., Zhou, G., Hui, J., Krogh, B., 2006. VigilNet: an integrated sensor network system for energy-efficient surveillance. ACM Transactions on Sensor Networks 2 (1), 1–38.

Hull, B., Bychkovsky, V., Zhang, Y., Chen, K., Goraczko, M., Miu, A., Shih, E., Balakrishnan, H., Madden, S., 2006. Cartel: a distributed mobile sensor computing system. In: Proc. ACM International Conference on Embedded Networked Sensor Systems , pp. 125–138.

IEEE standard for information technology–telecommunications and information exchange between systems–local and metropolitan area networks specific requirements part 15.4: wireless medium access control (MAC) and physical layer (PHY) specifications for low-rate wireless personal area networks (LR-WPANs), 2006.

Jennic JN5139, 2008. http://www.jennic.com/.

Juang, P., Oki, H., Wang, Y., Martonosi, M., Peh, L., Rubenstein, D., 2002. Energy-efficient computing for wildlife tracking: design tradeoffs and early experiences with zebranet. ACM SIGOPS Operating Systems Review 36 (5), 96–107.

Kargupta, H., Bhargava, R., Liu, K., Powers, M., Blair, P., Bushra, S., Dull, J., Sarkar, K., Klein, M., Vasa, M., Handy, D., 2004. VEDAS: a mobile and distributed data stream mining system for real-time vehicle monitoring. In: Proc. SIAM International Conference on Data Mining , pp. 300–311.

Lee, U., Zhou, B., Gerla, M., Magistretti, E., Bellavista, P., Corradi, A., 2006. Mobeyes: smart mobs for urban monitoring with a vehicular sensor network. IEEE Wireless Communications 13 (5), 52–57.

Li, M., Liu, Y., 2007. Underground structure monitoring with wireless sensor networks. In: Proc. International Symposium on Information Processing in Sensor Networks , pp. 69–78.

Liu, K., Li, M., Liu, Y., Li, M., Guo, Z., Hong, F., 2008. Passive diagnosis for wireless sensor networks. In: Proc. ACM International Conference on Embedded Networked Sensor Systems , pp. 113–126.

Sheu, J.P., Chen, P.C., Hsu, C.S., 2008. A distributed localization scheme for wireless sensor networks with improved grid-scan and vector-based refinement. IEEE Transactions on Mobile Computing 7 (September (9)), 1110–1123.

SIM300 module, 2008. http://www.sim.com/.

Tseng, Y.C., Wang, Y.C., Cheng, K.Y., Hsieh, Y.Y., 2007. iMouse: an integrated mobile surveillance and wireless sensor system. IEEE Computer 40 (6), 60–66.

uPatch300 module, 2008. http://www.fastraxgps.com/.

Wang, H., Estrin, D., Girod, L., 2003. Preprocessing in a tiered sensor network for habitat monitoring. In: EURASIP Journal on Applied Signal Processing, vol. 2003, pp. 392–401.

Wang, Y.C., Wu, F.J., Tseng, Y.C., 2010. Mobility management algorithms and applications for mobile sensor networks. Wireless Commununications and Mobile Computing.

Werner-Allen, G., Johnson, J., Ruiz, M., Lees, J., Welsh, M., 2005. Monitoring volcanic eruptions with a wireless sensor network. In: Proc. European Workshop on Wireless Sensor Networks , pp. 108–120. Werner-Allen, G., Lorincz, K., Ruiz, M., Marcillo, O., Johnson, J., Lees, J., Welsh, M., 2006. Deploying a wireless sensor network on an active volcano. IEEE Internet Computing 10, 18–25.

Xu, N., Rangwala, S., Chintalapudi, K.K., Ganesan, D., Broad, A., Govindan, R., Estrin, D., 2004. A wireless sensor network for structural monitoring. In: Proc. ACM International Conference on Embedded Networked Sensor Systems , pp. 13–24.

ZigBee specification version 2006, ZigBee document 064112, 2006.